# Acoustically detectable cellular-level lung injury induced by fluid mechanical stresses in microfluidic airway systems

**Dongeun Huh*†, Hideki Fujioka*, Yi-Chung Tung*, Nobuyuki Futai*, Robert Paine III‡§, James B. Grotberg*, and Shuichi Takayama*¶‖**

Departments of *Biomedical Engineering and ¶Macromolecular Science and Engineering, University of Michigan, Ann Arbor, MI 48109-2099; and ‡Division of Pulmonary and Critical Care Medicine, Department of Internal Medicine, University of Michigan, Ann Arbor, MI 48105

Edited by Howard A. Stone, Harvard University, Cambridge, MA, and accepted by the Editorial Board September 10, 2007 (received for review December 7, 2006)

**We describe a microfabricated airway system integrated with computerized air–liquid two-phase microfluidics that enables on-chip engineering of human airway epithelia and precise reproduction of physiologic or pathologic liquid plug flows found in the respiratory system. Using this device, we demonstrate cellular-level lung injury under flow conditions that cause symptoms characteristic of a wide range of pulmonary diseases. Specifically, propagation and rupture of liquid plugs that simulate surfactant-deficient reopening of closed airways lead to significant injury of small airway epithelial cells by generating deleterious fluid mechanical stresses. We also show that the explosive pressure waves produced by plug rupture enable detection of the mechanical cellular injury as crackling sounds.**

airway reopening | small airway epithelial cells | mechanical forces | microfluidic cell culture

The lung is a mechanically dynamic organ where epithelial cells constituting the luminal surface of the respiratory tract are continuously subjected to a variety of physical forces throughout development and adult life. Mechanical stresses have been shown to play an important role in regulating various functions of pulmonary epithelial cells such as growth (1–3), apoptosis (4–7), migration (8, 9), surfactant metabolism (1, 6, 10–12), synthesis of extracellular matrix proteins (11, 13), and transport of fluids and ions (12, 14, 15). Disruption of the local mechanical environment of the pulmonary epithelium often elicits abnormal cellular responses and can contribute to the pathogenesis and progression of various respiratory diseases (4, 5, 15–20).

In a variety of pulmonary diseases that can accompany surfactant dysfunction such as chronic obstructive pulmonary disease (21, 22), cystic fibrosis (23, 24), asthma (25), acute respiratory distress syndrome (26), pneumonia (27), and bronchiolitis (28), the impaired capabilities of pulmonary surfactant to lower surface tension render a viscous liquid film coating the small airway epithelium more prone to air–liquid two-phase instabilities. This situation often leads to the formation of liquid plugs across the airway lumen, which blocks small airways and impedes gas exchange in alveoli. Inflation of the lung during inhalation causes liquid plugs to propagate through airway tubes and rupture, reopening the occluded airways (29). In addition, transient pressure waves generated by plug rupture are believed to produce abnormal breath sounds known as respiratory crackles that are routinely used as an indicator of a wide range of respiratory disorders in clinics (30–33). Although clinically considered more as a symptom of respiratory diseases than as a cause, several theoretical investigations have suggested that the progression of liquid plugs or air bubbles during airway reopening can potentially generate deleterious fluid mechanical stresses characterized by large wall shear and normal stresses (34–39). There have also been experimental studies based on excised lungs or *in vivo* animal models that corroborate the theoretical predictions and demonstrate severe tissue damage in surfactant-deficient lungs as a result of repetitive airway reopening (40, 41). More recently, Gaver and colleagues (42–44) performed pioneering experimental investigations of micromechanical cellular injury induced by airway reopening. Using airway models that combined *in vitro* culture of pulmonary epithelial cell with semiinfinite air bubbles moving in a parallel-plate chamber, they revealed that mechanical stresses created by bubble progression caused significant cell damage and that pulmonary surfactant played a crucial role in mitigating the detrimental effect of reopening stresses. Their studies also provided valuable physical insights into airway reopening-induced cellular-level lung injury by showing that the magnitude of the pressure gradient near the bubble front, not the duration of stress exposure, determined the extent of cellular injury.

To further extend the work of Gaver and colleagues, we investigate mechanical injury of primary human small airway epithelial cells (SAECs) caused by the movement of liquid plugs with finite lengths in compartmentalized three-dimensional microfluidic systems. Reproduction of liquid plug flows observed during airway reopening is accomplished by a computerized microfluidic component that can dynamically switch microscale air–liquid two-phase flows. Furthermore, we examine the effect of the shortening and subsequent rupture of liquid plugs on airway epithelial cells. Through physiologic air–liquid interface culture that recapitulates the microenvironment of airway epithelial cells, the microengineered airway system enables the formation of differentiated airway epithelium *in vitro* that has appropriate secretory function and structural integrity. Using this device, we demonstrate injurious response of SAECs to propagation and rupture of finite liquid plugs that simulate the reopening of closed airways afflicted with surfactant deficiency. We show that there is a higher risk of cellular injury when propagating liquid plugs become very thin and subsequently

Author contributions: D.H., R.P., J.B.G., and S.T. designed research; D.H. performed research; H.F., Y.-C.T., N.F., and J.B.G. contributed new reagents/analytic tools; D.H., H.F., Y.-C.T., J.B.G., and S.T. analyzed data; and D.H. and S.T. wrote the paper.

The authors declare no conflict of interest.

This article is a PNAS Direct Submission. H.A.S. is a guest editor invited by the Editorial Board.

†Present address: Vascular Biology Program, Departments of Pathology and Surgery, Harvard Medical School and Children's Hospital, Boston, MA 02115.

§Present address: Department of Internal Medicine and Division of Pulmonary and Critical Care Medicine, University of Utah School of Medicine, Salt Lake City, UT 84132.

‖To whom correspondence should be addressed at: Department of Biomedical Engineering, University of Michigan, 2200 Bonisteel Boulevard, 2115 Gerstacker, Ann Arbor, MI 48109-2099. E-mail: takayama@umich.edu.

This article contains supporting information online at www.pnas.org/cgi/content/full/0610868104/DC1.

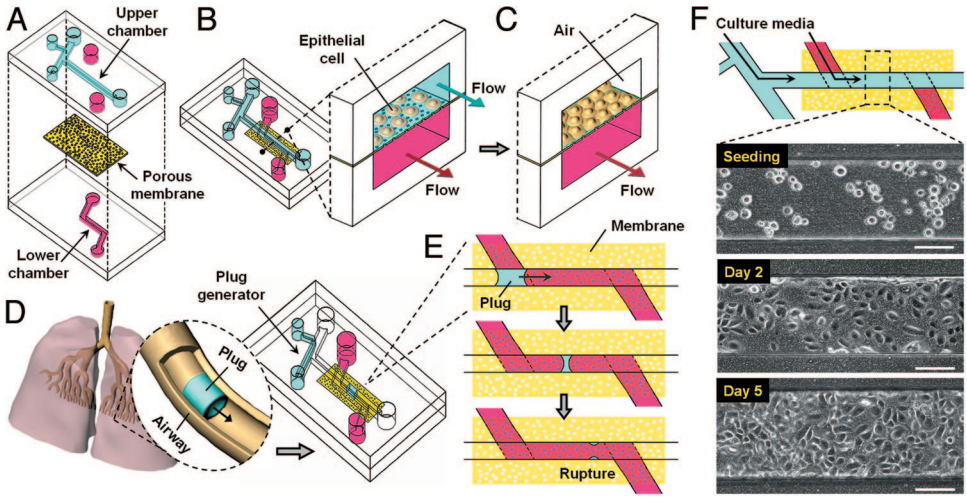


**Fig. 1.** Compartmentalized microfluidic airway systems. (*A*) The microfabricated small airways are comprised of PDMS upper and lower chambers sandwiching a porous membrane. (*B*) SAECs are grown on the membrane with perfusion of culture media in both upper and lower chambers until they become confluent. (*C*) Once confluence is achieved, media are removed from the upper chamber, forming an air–liquid interface over the cells. During air–liquid interface (ALI) culture, the cells are fed basally and undergo cellular differentiation. (*D*) Physiologic airway closure is recreated in the microfluidic system by exposing the differentiated cells to plug flows. (*E*) Liquid plugs created in a plug generator progress over a monolayer of the epithelial cells and rupture in the downstream region, reopening the *in vitro* small airways. (*F*) SAECs seeded into the upper chamber attach to a membrane within 5 hr after seeding in the absence of fluid flows. Continuous perfusion of media supports cell growth into monolayers with typical epithelial appearance. Confluence is reached ≈6 days after seeding, at which time ≈95% of the membrane surface inside the microchannel is uniformly covered with SAECs. (Scale bars: 150 $\mu$m.)

rupture. Furthermore, we demonstrate that the mechanical injury events due to airway reopening can be acoustically detected as crackling sounds produced by rupture of liquid plugs.

The microfluidic airway system consists of two poly(dimethylsiloxane) (PDMS) chambers separated by a thin polyester membrane with 400-nm pores (Fig. 1*A*). Upper and lower chambers correspond to apical (airway lumen) and basal compartments of airway epithelium, respectively. The porous membrane mimics an *in vivo* basement membrane and provides transparent supports for cell attachment and growth. The size of the microchannels (300 $\mu$m in width and 100 $\mu$m in height) was chosen to approximate the diameters of distal conducting airways and respiratory bronchioles. Transport of fluids and solutes between chambers is limited to diffusion through membrane pores, permitting spatially selective and independent microfluidic transport in each chamber without leakage. The compartmentalized nature of the channel architecture and fluid delivery enables tissue engineering of airway epithelial cells to produce a confluent monolayer that closely resembles native airway tissue. As the first step of microfluidic culture, SAECs are seeded into the upper chamber and cultured on the porous membrane while both apical and basal sides are perfused with culture media (Fig. 1*B*). Once the cells reach confluence, their apical surface is exposed to an air–liquid interface established by removing media from the upper chamber, and the monolayer is fed only on the basolateral side (Fig. 1*C*). This configuration induces cellular differentiation that causes airway epithelial cells to express morphological and secretory phenotypes matching those found *in vivo* (45–47).

The monolayer of fully differentiated SAECs is then subjected to different types of fluid flows. For instance, air flow can be driven over the monolayer at slow speeds to simulate normal breathing situations. Single-phase liquid flows through the upper chamber can be used to recreate the motion of liquid during total liquid ventilation (48) or fetal breathing movements in the developing lung (49). For investigation of lung injury during airway reopening, the prepared cells are exposed to plug propagation and rupture to reproduce *in vivo* airway reopening in the microfabricated *in vitro* small airway (Fig. 1*D*). Liquid plugs are created by a plug generator integrated with the upper chamber and propagate over the epithelial cells. As liquid plugs move down the microchannel, they shorten as a result of the deposition of a trailing film (29) and eventually rupture in the downstream region (Fig. 1*E*).

## Results and Discussion

Under liquid perfusion culture conditions, the SAECs exhibited a monolayer growth pattern and remained proliferative over a period of 6 days (Fig. 1*F*) to produce a confluent monolayer with ≈90% viability, as assessed by live/dead staining (Fig. 2*A*). When grown at an air–liquid interface, the SAECs lost their proliferative capacity, presumably because of the initiation of cellular differentiation as well as contact inhibition. Air–liquid interface culture over 3 weeks resulted in no significant change in viability (Fig. 2*B*). The cells in the regions not adjoining the lower chamber, however, were found to be dead (Fig. 2*C*), illustrating a vital role of basal feeding in sustaining the SAECs during prolonged periods of air–liquid interface culture. Immunohistochemical quantification of Clara cell 10-kDa protein (CC10), a known marker of differentiated and biochemically functional airway epithelial cells (45, 50), revealed a marked increase in CC10 upon exposure of the cells to an air–liquid interface (Fig. 2*D*). The concentration of CC10 increased over the first 9 days and decreased gradually throughout the rest of the culture period, consistent with the observations reported in macroscopic airway epithelial cell cultures (45). Liquid perfusion culture resulted in no detectable CC10 expression regardless of its duration.

Closure and reopening of microfluidic small airways are achieved by dynamically switching air–liquid two-phase flows in a microfabricated plug generator integrated with the culture chamber. Initially, liquid is injected into the plug generator and focused by air flows to form a stable stratification of air and liquid (Fig. 3*A*) (51, 52). When air is valved off, the liquid stream spreads instantaneously and progresses gradually into the culture chamber (Fig. 3*B*). Recovery of air flow reestablishes the stratified two-phase flows and "pinches off" the liquid column advancing to the culture chamber, which results in the formation

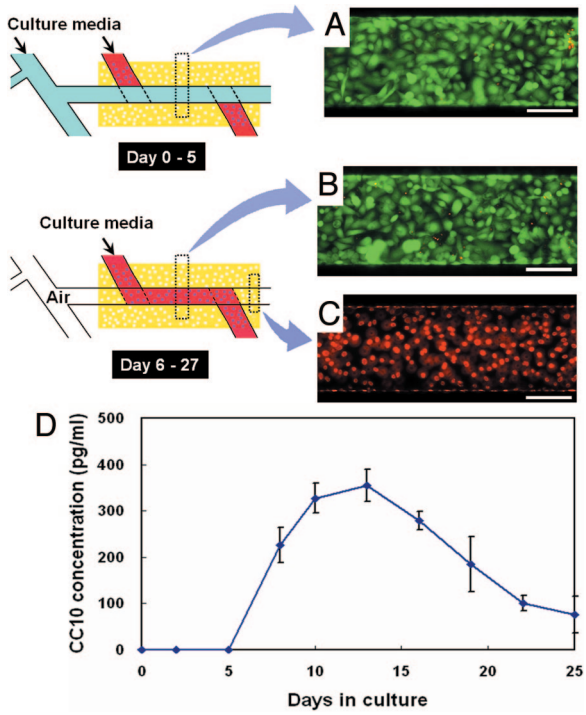


**Fig. 2.** Microfluidic production of *in vitro* small airway tissue. Liquid perfusion culture over 6 days generates a confluent monolayer of SAECs with high viability (mean ± SD = 90.4 ± 5.17%), as illustrated in *A*. Green and red represent live and dead cells, respectively. (*B*) During ALI culture lasting 3 weeks, the steady flow of culture media in the lower chamber sustains the cells on the membrane, maintaining high viability (87.6 ± 3.77%). (*C*) The cells in the areas without basal feeding die from starvation, leading to no detection of live cells. (Scale bars: 150 $\mu$m.) (*D*) ALI culture induces differentiation of SAECs as indicated by the production of CC10. The level of protein secretion is not measurable during liquid perfusion culture and increases considerably within 9 days after the formation of an air–liquid interface. Data represent mean ± SD of samples collected from three independent experiments ($n = 3$).

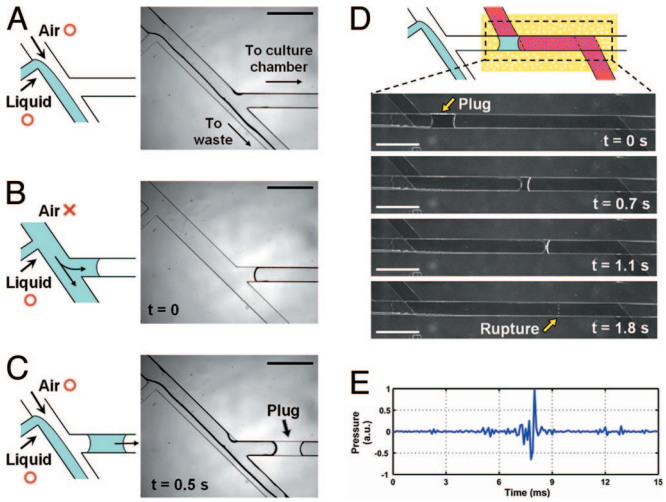


**Fig. 3.** Formation, propagation, and rupture of liquid plugs generated by dynamic fluidic switching in a microfabricated plug generator. (*A*) In the plug generator, injected liquid is stably focused by air to form stratified air–liquid two-phase flows. Liquid exits to a waste outlet. (*B*) Blockage of air causes liquid to enter the culture chamber. (*C*) Subsequently, air flow is resumed and original two-phase stratification is recovered, resulting in the formation of a liquid plug in the culture chamber. (*D*) As liquid plugs move through the upper chamber, they become shorter because of volume loss and ultimately rupture in the downstream region. (Scale bars: 1 mm.) (*E*) Plug rupture in microchannels produces pressure waves resembling transient acoustic waves of respiratory crackles. Note that the time scale in the pressure plot is expanded over the period of 15 ms to emphasize the dynamics of rapid pressure fluctuations caused by plug rupture.

and propagation of a liquid plug in the airway microchannel (Fig. 3*C*). During propagation, the liquid plug loses its volume by depositing liquid onto the channel wall from its rear meniscus and becomes shorter until it ruptures in the downstream region (Fig. 3*D*). The length and propagation speed of liquid plugs can be controlled by changing the duration of air blockage and the flow rate of air, respectively [see supporting information (SI) Fig. 5]. This integrated component provides unique capabilities to precisely mimic fluid motions characteristic of airway reopening, which would be difficult to achieve by using traditional tissue culture methods or *ex vivo* airway models based on excised lungs.

Rupture of liquid plugs in the microfluidic small airways generated transient pressure waves similar to those producing respiratory crackles that can be auscultated in routine clinical settings to identify airway reopening. We used a laser vibrometer (53) to detect out-of-plane motion of microchannel walls caused by pressures during plug rupture. The measurements revealed that large pressure pulses were generated in coincidence with rupture events inside the airway microchannel. The resulting pressure waveforms had small initial deflections followed by spikes with larger amplitudes (Fig. 3*E*), which closely resembles the patterns found in the acoustic waveforms of naturally occurring crackles as shown by time-expanded waveform analysis (30, 33, 54). The duration of an initial deflection and the total duration of waves were approximated to be 0.5 ms and 1.5 ms, respectively. These values are fairly similar to the acoustic parameters of fine crackles where the mean time duration of an initial deflection and the first two cycles of the waveform are typically 0.5 ms and 5 ms, respectively (30, 33). These observations illustrate that our system enables *in vitro* recreation of not only fluid dynamics of airway reopening, but also its essential acoustic characteristics that are clinically more relevant (actual sounds are provided as SI Soundtrack 1).

To drive liquid plugs, we used physiological flow rates of air estimated from typical tidal volumes and the Weibel model (55), which prompted plugs to move at a mean velocity of ≈1.5 mm/s in the microchannel. As a control condition, differentiated SAECs were exposed to single-phase liquid flows at ≈1.5 mm/s, which may be relevant to fetal breathing in late gestation or total liquid ventilation. This resulted in no discernible injury of the cells, as indicated by their viability (≈85%) (Fig. 4*A*). In addition, air flow over a monolayer of differentiated SAECs at physiological velocities simulating normal breathing did not cause cellular damage (data not shown). When the monolayer was subjected to 10 events of plug propagation and subsequent rupture over a period of 10 min (1 event per min), however, there was a significant increase ($P < 0.0001$, $n = 10$) in the number of membrane-compromised cells, and viability was reduced by ≈24% (Fig. 4*B*). The fraction of injured cells increased proportionally with escalating doses of fluid mechanical stresses imposed by 50 and 100 events of plug progression and rupture over 10 min (Fig. 4 *C–E*) ($P < 0.0001$, $n = 10$). These observations suggest that the two-phase fluid motion characteristic of airway reopening generates a substantial amount of deleterious mechanical stresses and causes airway injury. Considering that the cells did not exhibit significant injurious response after a single reopening event (data not shown) and that the mechanical stresses imposed by a single propagation/rupture remained the same throughout the experiments, these results may also indicate the important role of repetitive reopening events in inducing and exacerbating mechanical cellular injury.

We estimated mechanical stresses acting on the cell surface by computationally investigating the flow field created by a liquid

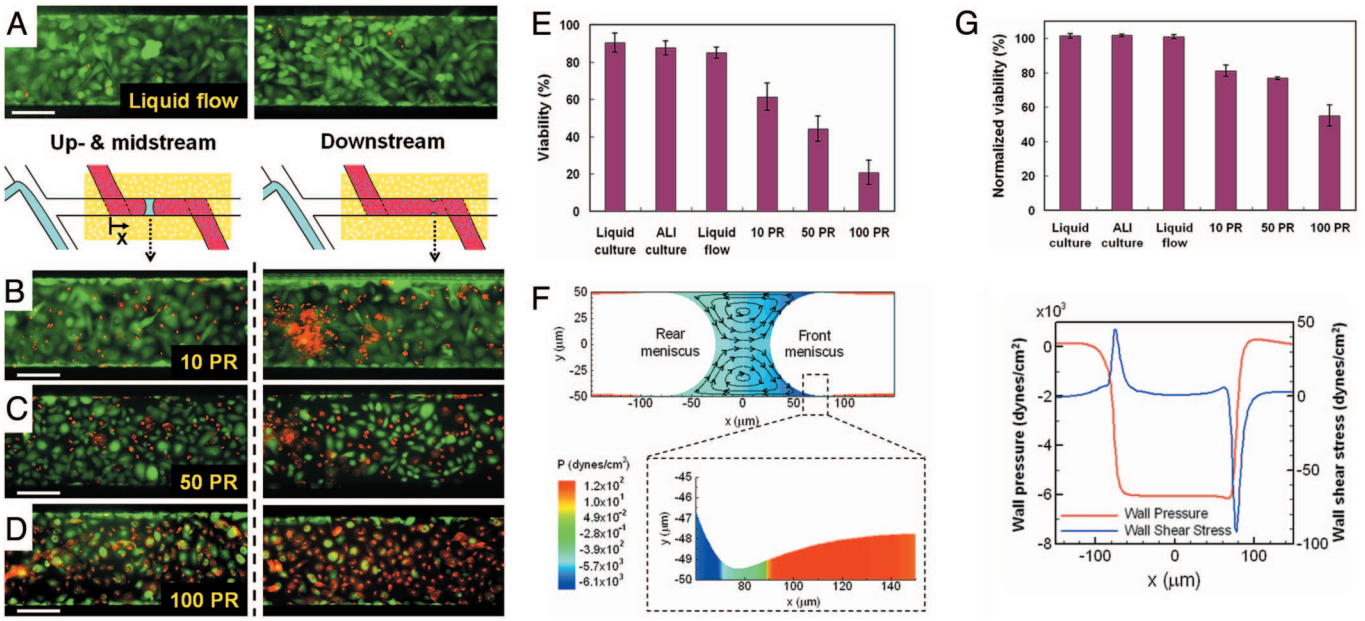


**Fig. 4.** Cellular injury caused by propagation and rupture of liquid plugs. (*A*) Single-phase liquid flows do not damage differentiated SAECs. Exposure of the cells to propagation and subsequent rupture of liquid plugs results in progressively larger numbers of injured cells, as shown in *B–D*. PR represents the number of plug propagations and subsequent ruptures over a period of 10 min. ''Upstream and midstream'' and ''downstream'' areas range from $x = 0$ to 2.9 mm and from $x = 2.9$ mm to 3.7 mm, respectively. (Scale bars: 150 $\mu$m.) (*E*) The extent of cellular damage is elevated with the increasing number of reopening events. (*F*) Numerical simulation reveals that propagating liquid plugs form recirculation in the core region and generate large gradients of wall pressure and wall shear stress in the precursor film where the film thickness is the smallest. (*G*) Downstream viability normalized by the percent viability of cells in the upstream and midstream regions decreases significantly in the presence of reopening flows, suggesting that more deleterious mechanical stresses are generated in the vicinity of the site of plug rupture.

plug (34) moving in two-dimensional parallel-plate channels. In situations matching the experimentally defined channel geometry and flow conditions (channel height of 100 $\mu$m, propagation speed of $\approx$1.5 mm/s), there exist abnormally large gradients of wall pressure and wall shear stress in the area of smallest film thickness, known as a capillary wave, where the front meniscus converges to a precursor film (Fig. 4*F*). The stresses and stress gradients exerted by the front meniscus of a liquid plug are larger than those generated by the rear meniscus, suggesting that cellular injury due to plug propagation is mainly a result of the movement of the front meniscus of a liquid plug. Considering that the length of a single cell ($\approx$40 $\mu$m) is greater than that of the capillary wave, the maximum pressure drop and shear stress change within a cell can be estimated to be the largest change in the magnitude of the wall pressure and shear stress in the capillary wave region, which are 6,454.9 dynes/cm$^2$ and 97.58 dynes/cm$^2$, respectively. It should be noted, however, that these values may change because of the factors that have not been taken into account in our study, such as pulmonary surfactant (42, 43, 44, 56, 57), airway compliance (35–37), and non-planar topography of the airway wall resulting from the protrusion of airway epithelial cells (38).

It is noted that there were larger numbers of injured cells in the downstream regions where liquid plugs became very thin and subsequently ruptured. In the presence of plug flows, viability in the downstream area normalized with respect to the percent fraction of live cells in the domain spanning the upstream and midstream areas decreased significantly (19–47% more death; $P < 0.0001$) as compared with that in controls—liquid perfusion culture, ALI culture, and exposure of cells to single-phase liquid flows (Fig. 4*G*). This observation is indicative of detrimental mechanical stresses in the downstream region that are sufficiently larger than those produced by plug propagation in the upstream and midstream regions, illustrating a higher risk of cellular injury due to the unique stress environment created at the site of plug rupture and its vicinity. As the plug length becomes very small shortly before plug rupture takes place, the interaction between the leading and trailing menisci may increase interfacial curvature, which can elevate the pressure drop across the air–liquid interface and therefore impose larger mechanical stresses on the cells. The large curvature of the interface after plug rupture and subsequent drainage of fluid into the neighboring liquid film are also expected to be more damaging to the epithelial cells.

These results also reveal findings that distinguish our system from the previous *in vitro* reopening models (42–44) where nondifferentiated and immortalized epithelial cells grown on glass substrates in liquid culture are subjected to the air–liquid interface of a progressing semiinfinite air bubble to simulate the first breaths of a newborn. (*i*) Despite larger mechanical stresses generated by the movement of a finite liquid plug, airway epithelium produced by physiologic air–liquid interface culture of primary epithelial cells is much more resistant to injury induced by plug propagation under the conditions that would cause severe damage of cells in the previous *in vitro* models. This is presumably because of air–liquid interface culture-induced cellular differentiation that may strengthen monolayer integrity via formation of tight junctions and desmosomes (45, 46) (see *SI Text*). It is also possible that cellular production of secretory proteins initiated and maintained by air–liquid interface culture may serve to protect the cells. (*ii*) The microfluidic airway system enables us to demonstrate the important role of one of the possible final steps of reopening events—progression of very thin liquid plugs and their subsequent rupture—in promoting mechanical tissue injury during airway reopening. This has not been possible to address in the previous models. Our study, however, does not consider the effect of pulmonary surfactant and thus is limited in simulating the reopening stresses that would exist in the airway system with surfactant dysfunction. Normal surfactant function would reduce surface tension and

the peaks of wall pressure and wall shear stress (58), providing a degree of protection to cells from mechanical damage associated with plug propagation and rupture. It should also be noted that in the same way that surfactants stabilize foams, pulmonary surfactant may stabilize thinning plugs to form lamellae that resist rupture.

From a clinical perspective, our results imply that respiratory crackles created by airway reopening may be associated with mechanical airway injury in various respiratory diseases with impaired capabilities of surfactant to lower surface tension. Our system is limited in reproducing structural flexibility of airway epithelium that may serve to dampen the detrimental effect of reopening-induced mechanical stresses *in vivo*. Pathological conditions that cause airway remodeling with increased connective tissue in the airway wall, which often accompany surfactant dysfunction [especially in asthma (59–61) and chronic obstructive pulmonary disease], however, might stiffen the airway wall and render the epithelial cells more prone to mechanical injury, as demonstrated in this work. Our studies provide insights into understanding physiological nature of crackles beyond a symptom of pulmonary disorders involving edema, infection, or inflammation. Our demonstrations raise the possibility that airway reopening, which is manifest as crackles, can mechanically aggravate pulmonary diseases exhibiting surfactant dysfunction, which may lead to the severe lung injuries often found in such diseases.

These findings are consistent with the deleterious effects of reopening plug flows observed by previous theoretical and experimental studies, confirming the crucial role of fluid mechanical stresses in understanding the onset and exacerbation of physical force-induced lung injuries. Our investigation also highlights a multipronged approach combining microfluidics and microfabrication with tissue engineering to developing robust *in vitro* airway models. The microfluidic airway system provides highly controllable and readily accessible physiologic pulmonary environments tailored for lung epithelial cells and respiratory flows of interest. We believe that our approach will enhance the current understanding of cellular response to complex pulmonary mechanical forces and potentially contribute to the designing of strategies for treating and preventing lung injuries of fluid mechanical origin.

## Materials and Methods

**Microfluidic Cell Culture.** Primary SAECs and serum-free SAEC basal medium supplemented with growth factors were obtained from Cambrex Life Sciences. Before use in microchannels, the cells were maintained in the complete growth media and cultured in 25-$cm^2$ flasks according to the manufacture's protocols. Cells were used for microfluidic culture after the first or second subculture. Before cell seeding, airway microchannels were sterilized by UV irradiation, filled with media, and preincubated overnight. SAECs were seeded at $10^5 \sim 10^6$ cells per $cm^2$ into the upper chamber, and liquid flows were completely stopped to facilitate cell attachment. After 5 hr, steady flows of culture media were driven by a syringe pump at 25 $\mu$l/hr in each chamber. The microfluidic culture was maintained at 37°C in a humidified incubator with 5% $CO_2$ in air. Once confluence was achieved, culture media were aspirated from the upper chamber to establish an air–liquid interface at the apical surface of a monolayer. During air–liquid interface culture, culture media were driven at 15 $\mu$l/hr through the lower chamber.

**Immunohistochemical Detection of CC10.** During liquid perfusion culture, media perfused through an upper chamber were collected from the outlet of the upper chamber every 3 days and stored frozen at −20°C for later analysis. During air–liquid interface culture, the apical surface of a monolayer was washed with 100 $\mu$l of culture media every 3 days, and the resulting liquids from the outlet were stored in the same manner. A human Clara cell protein ELISA kit was purchased from United States Biological to quantify the concentration of CC10 in the collected samples. Briefly, conditioned media were injected into microtiter wells coated with polyclonal anti-human Clara cell protein antibodies. After incubation and a washing, polyclonal anti-human Clara cell protein antibodies labeled with biotin were added and incubated. The wells were washed and, subsequently, streptavidin-horseradish peroxidase complex was added to bind to biotin. After incubation and the last washing step, the conjugate reacted with substrate $H_2O_2$-tetramethylbenzidine. A commercial ELISA reader was used to measure the absorbance of the resulting product at 450 nm.

**Viability Assay.** The upper chamber was filled with a mixture solution containing calcein AM (2 $\mu$M in culture media) and ethidium homodimer-1 (4 $\mu$M) and incubated in a culture incubator for 10 min, after which the upper chamber was examined by fluorescence microscopy. For the assessment of cellular damage due to plug flows, fluorescence staining was performed ≈20 min after the termination of experiments so that small and compensable membrane disruptions were allowed to reseal and the assay could capture permanently injured cells exclusively. Cellular viability was quantified by the percentage of calcein AM-labeled cells averaged over 10 different observation areas of the upper chamber from multiple independent experiments. Obtained data were represented as mean ± SD. We used analysis of variance (ANOVA) followed by post hoc Tukey's multiple comparison test (Fig. 4*E*) or two-tailed Student's *t* test (Fig. 4*G*) to determine statistical significance.

**Generation of Liquid Plugs.** Air and liquid flows were driven by compressed air and a syringe pump, respectively. Air flows were regulated by a solenoid-operated high-speed (response time of ≈25 ms) pinch valve controlled by a personal computer. The valve was used to close and subsequently reopen silicone tubing connecting a compressed air tank to the airway microchannels. PBS was used as working liquid and injected into the microchannel at 10 ml/hr.

We thank Dr. Shalini Anthwal for assistance in cell culture, Dr. Karl Grosh for providing access to a laser vibrometer, and Dr. Joseph L. Bull and Dr. Katsuo Kurabayashi for comments on designing experiments. This work was supported by National Institutes of Health Grant HL084370-01, the Whitaker Foundation, the National Aeronautics and Space Administration, and National Science Foundation Grant BES-0238625. D.H. acknowledges a Horace H. Rackham Predoctoral Fellowship from the University of Michigan.

1. Scott JE, Yang SY, Stanik E, Anderson JE (1993) *Am J Respir Cell Mol Biol* 8:258–265.
2. Liu M, Skinner SJM, Xu J, Han RNN, Tanswell AK, Post M (1992) *Am J Physiol* 263:L376–L383.
3. Schittny JC, Miserocchi G, Sparrow MP (2000) *Am J Respir Cell Mol Biol* 23:11–18.
4. Tschumperlin DJ, Margulies SS (1998) *Am J Physiol* 275:L1173–L1183.
5. Tschumperlin DJ, Oswari J, Margulies SS (2000) *Am J Respir Crit Care Med* 162:357–362.
6. Edwards YS, Sutherland LM, Power JHT, Nicholas TE, Murray AW (1999) *FEBS Lett* 448:127–130.
7. Hammerschmidt S, Kuhn H, Grasenack T, Gessner C, Wirtz H (2004) *Am J Respir Cell Mol Biol* 30:396–402.
8. Savla U, Waters CM (1998) *Am J Physiol* 274:L883–L892.
9. Waters CM, Glucksberg MR, Lautenschlager EP, Lee CW, Van Matre RM, Warp RJ, Savla U, Healy KE, Moran B, Castner DG, *et al.* (2001) *J Appl Physiol* 91:1600–1610.
10. Sanchez-Esteban J, Cicchiello LA, Wang YL, Tsai SW, Williams LK, Torday JS, Rubin LP (2001) *J Appl Physiol* 91:589–595.
11. Nakamura T, Liu MY, Mourgeon E, Slutsky A, Post M (2000) *Am J Physiol* 278:L974–L980.

12. Wirtz HRW, Dobbs LG (1990) *Science* 250:1266–1269.
13. Xu J, Liu MY, Post M (1999) *Am J Physiol* 276:L728–L735.
14. Waters CM, Ridge KM, Sunio G, Venetsanou K, Sznajder JI (1999) *J Appl Physiol* 87:715–721.
15. Olver RE, Walters DV, Wilson SM (2004) *Annu Rev Physiol* 66:77–101.
16. Vlahakis NE, Schroeder MA, Limper AH, Hubmayr RD (1999) *Am J Physiol* 277:L167–L173.
17. Liu MY, Tanswell AK, Post M (1999) *Am J Physiol* 277:L667–L683.
18. Swartz MA, Tschumperlin DJ, Kamm RD, Drazen JM (2001) *Proc Natl Acad Sci USA* 98:6180–6185.
19. Choe MM, Sporn PHS, Swartz MA (2006) *Am J Respir Cell Mol Biol* 35:306–313.
20. Choe MM, Swartz MA (2003) *Am J Physiol* 285:L427–L433.
21. Hogg JC, Chu F, Utokaparch S, Woods R, Elliott WM, Buzatu L, Cherniak RM, Rogers RM, Sciurba FC, Coxson HO, *et al.* (2004) *N Engl J Med* 350:2645–2653.
22. Guérin C, Lemasson S, de Varax R, Milic-Emili J, Fournier G (1997) *Am J Respir Crit Care Med* 155:1949–1956.
23. Griese M, Essl R, Schmidt R, Rietschel E, Ratjen F, Ballmann M, Paul K (2004) *Am J Respir Crit Care Med* 170:1000–1005.
24. Tirouvanziam R, Khazaal I, Peault B (2002) *Am J Physiol* 283:L445–L451.
25. in 't Veen JC, Beekman AJ, Bel EH, Sterk PJ (2000) *Am J Respir Crit Care Med* 161:1902–1906.
26. Baker CS, Evans TW, Randle BJ, Haslam PL (1999) *Lancet* 353:1232–1237.
27. Gunther A, Siebert C, Schmidt R, Ziegler S, Grimminger F, Yabut M, Temmesfeld B, Walmrath D, Morr H, Seeger W (1996) *Am J Respir Crit Care Med* 153:176–184.
28. Dargaville PA, South M, McDougall PN (1996) *Arch Dis Child* 75:133–136.
29. Grotberg JB (2001) *Annu Rev Biomed Eng* 3:421–457.
30. Piirila P, Sovijarvi ARA (1995) *Eur Respir J* 8:2139–2148.
31. Petak F, Habre W, Babik B, Tolnai J, Hantos Z (2006) *Eur Respir J* 27:808–816.
32. Alencar AM, Majumdar A, Hantos Z, Buldyrev SV, Stanley HE, Suki B (2005) *Physica A* 357:18–26.
33. Pasterkamp H, Kraman SS, Wodicka GR (1997) *Am J Respir Crit Care Med* 156:974–987.
34. Fujioka H, Grotberg JB (2004) *J Biomech Eng* 126:567–577.
35. Gaver DP, Halpern D, Jensen OE, Grotberg JB (1996) *J Fluid Mech* 319:25–65.
36. Jensen OE, Horsburgh MK, Halpern D, Gaver DP (2002) *Phys Fluids* 14:443–457.
37. Halpern D, Naire S, Jensen OE, Gaver DP (2005) *J Fluid Mech* 528:53–86.
38. Jacob AM, Gaver DP (2005) *Phys Fluids* 17:031502.
39. Heil M (2000) *J Fluid Mech* 424:21–44.
40. Muscedere JG, Mullen JBM, Gan K, Slutsky AS (1994) *Am J Respir Crit Care Med* 149:1327–1334.
41. Taskar V, John J, Evander E, Robertson B, Jonson B (1997) *Am J Respir Crit Care Med* 155:313–320.
42. Bilek AM, Dee KC, Gaver DP (2003) *J Appl Physiol* 94:770–783.
43. Kay SS, Bilek AM, Dee KC, Gaver DP (2004) *J Appl Physiol* 97:269–276.
44. Gaver DP, Jacob AM, Bilek AM, Dee KC (2006) in *Ventilator-Induced Lung Injury*, eds Dreyfuss D, Saumon G, Hubmayr RD (Taylor & Francis, New York), pp 157–203.
45. You Y, Richer EJ, Huang T, Brody SL (2002) *Am J Physiol* 283:L1315–L1321.
46. Davidson DJ, Kilanowski FM, Randell SH, Sheppard DN, Dorin JR (2000) *Am J Physiol* 279:L766–L778.
47. Yoon JH, Gray T, Guzman K, Koo JS, Nettesheim P (1997) *Am J Respir Cell Mol Biol* 16:724–731.
48. Foley DS, Brah R, Bull JL, Brant DO, Grotberg JB, Hirschl RB (2004) *ASAIO J* 50:485–490.
49. Del Riccio V, Van Tuyl M, Post M (2004) *Pediatr Res* 55:183–189.
50. Armit CJ, O'Dea S, Clarke AR, Harrison DJ (2002) *BMC Cell Biol* 3:27.
51. Huh D, Tung YC, Wei HH, Grotberg JB, Skerlos SJ, Kurabayashi K, Takayama S (2002) *Biomed Microdevices* 4:141–149.
52. Huh D, Tkaczyk AH, Bahng JH, Chang Y, Wei HH, Grotberg JB, Kim CJ, Kurabayashi K, Takayama S (2003) *J Am Chem Soc* 125:14678–14679.
53. White RD, Grosh K (2005) *Proc Natl Acad Sci USA* 102:1296–1301.
54. Hoevers J, Loudon RG (1990) *Chest* 98:1240–1243.
55. Weibel ER, Gomez DM (1962) *Science* 137:577–585.
56. Ghadiali SN, Gaver DP (2000) *J Appl Physiol* 88:493–506.
57. Yap DYK, Gaver DP (1998) *Phys Fluids* 10:1846–1863.
58. Fujioka H, Grotberg JB (2005) *Phys Fluids* 17:082102.
59. Hohlfeld JM (2001) *Respir Res* 3:4.
60. Haczku A, Atochina EN, Tomer Y, Cao Y, Campbell C, Scanlon ST, Russo SJ, Enhorning G, Beers MF (2002) *Am J Physiol* 283:L755–L765.
61. Hohlfeld JM, Ahlf K, Enhorning G, Balke K, Erpenbeck VJ, Petschallies J, Hoymann HG, Fabel H, Krug N (1999) *Am J Respir Cell Mol Biol* 159:1803–1809.